CASE 1: Synthetic Jets in Quiescent Air

C. S. Yao, F. J. Chen, D. Neuhart, and J. Harris

Flow Physics & Control Branch, NASA Langley Research Center, Hampton, VA 23681-2199

Introduction

An oscillatory jet with zero net mass flow is generated by a cavity-pumping actuator. Among the three test cases selected for the Langley CFD validation workshop to assess the current CFD capabilities to predict unsteady flow fields, this basic oscillating jet flow field is the least complex and is selected as the first test case. Increasing in complexity, two more cases studied include jet in cross flow boundary layer and unsteady flow induced by suction and oscillatory blowing with separation control geometries.

In this experiment, velocity measurements from three different techniques, hot-wire anemometry, Laser Doppler Velocimetry (LDV) and Particle Image Velocimetry (PIV), documented the synthetic jet flow field. To provide boundary conditions for computations, the experiment also monitored the actuator operating parameters including diaphragm displacement, internal cavity pressure, and internal cavity temperature.

Experiment Setup

Synthetic jet actuator

The synthetic jet actuator for this experiment was based on an earlier design studied in detail by Chen et al (2000)[1] and Chen (2002)[2]. The jet exit slot of the actuator (Fig. 1) is 0.05 inches wide and 1.4 inches long. The slot width was larger than the previous design to allow velocity profiles across the slot to be properly resolved. The actuator is flush mounted on an aluminum plate at the floor, and is covered by a glass enclosure, 2 x 2 x 2 feet in dimension and ¼ inch thick. The glass enclosure isolates the synthetic jet flow from the ambient air and serves to contain the seeding particles as well. A sliding door on the glass panel provides access for seeding and the hot-wire probe. The jet is located at the center of the floor, and the slot is parallel to the glass sidewall.

The actuator has a Plexiglas housing with a narrow cavity beneath the slot. The jet flow was driven by a single piezo-electric diaphragm, 2" in diameter, mounted on one side of a narrow cavity. The piezo diaphragm was driven at 445 Hz, which was selected to operate away from the cavity resonant frequency near 500 Hz. Figure 2 shows the output of the actuator as a function of the forcing frequency. An o-ring seal, 1.85" in diameter, is clamped between the diaphragm and the actuator cavity. Maximum jet velocity generated could reach 30 ~ 50 m/s, depending on the actuator performance, and the aging of actuator. In daily test, there was no performance degrading with time. The actuator did show a gradual decreasing of the pressure level with a long period of usage over months. Sometime, the diaphragm needed to be replaced due to the cabling faults.

Actuator parameters

Three actuator operating parameters including diaphragm displacement, cavity pressure and cavity temperature, were measured to monitor the actuator performance, and provide boundary conditions for computation and actuator modeling (Fig. 3). A fiber optics displacement sensor is installed to measure the diaphragm displacement at the center of the piezo-electric disc. The fiber probe was calibrated in-situ using a micrometer. The displacement measured ranges between +0.2 ~ -0.4 mm, for in-ward and out-ward displacements. A dynamic pressure transducer installed at the center of the sidewall (the fixed wall) opposite of the diaphragm to measure the instantaneous cavity pressure waveforms. A thermal couple device is installed at the bottom of the cavity to monitor the internal temperature.

Hot-wire measurements

Hot-wire Anemometry provides a single point in space and a time history measurements of the velocity component perpendicular to the sensing wire. In the current setup, hot-wire measurements were made with a constant-temperature anemometer (CTA) and a single-sensor hot-wire probe. The sensing element of the hot-wire probe, 5 μm in diameter and 1.25 mm long, is a platinum-plated tungsten wire operated at an overheat ratio of 1.8. The probe was mounted perpendicular to the floor with the sensing element located at the center of the slot and parallel to the long axis of the slot. Measurements were taken at 47 stations with height ranges to 50 mm above the slot. A hot-wire probe support was mounted on a translation stage with a computer-controlled traversing system installed on the exterior of the glass enclosure. A slotted opening on the sidewall provides the access into the glass enclosure.

The hot-wire probe was calibrated with a commercial desktop calibration unit. The signals from the CTA outputs were sampled at 100 kHz with 16384 data points recorded at each station. For a forcing frequency of 445 Hz, there are 72 periods of waveform recorded. Within each period of the driving cycle there were 225 data points. Seventy-two samples were averaged to compute the phase-locked statistics. Hot-wire signals were de-rectified to obtain negative velocities during the actuator suction cycle at lower stations. Uncertainty was +/- 2.5 % for measurements of heights of 5 mm or higher and +/- 6 % for lower stations near the solid surface.

Laser Doppler Velocimetry measurements

Similar to hot-wire measurements, LDV is single point in space measurement technique. LDV signals provide a velocity record and the corresponding particle arrival time whenever a valid signal is detected. In this test, a LDV system was set up to measure the vertical jet velocity and its decay along the centerline of the slot. Vertical velocity measurements were made at 47 locations above the rectangular slot between 0 to 70 mm. The transmitted laser beams from a fiber optic probe were projected through the glass sidewall in a direction parallel to the long axis of the rectangular jet slot, and in a vertical plane. The crossing point of the two laser beams, which is the LDV sample volume, was centered over the center of the slot, both longitudinally and laterally. The scattered light from the seeding particles was collected by a second fiber optic probe, which was located in the forward-scatter direction, 50 degrees off of the direct forward scatter axis.

The seeding particles were 0.9-micron polystyrene latex spheres (PSL, specific gravity at 1.04), suspended in 200-proof ethanol. Based on a first–order estimation, particles ~ O(1 μm) follow the flow well at the applied frequency. The laser was an argon-ion laser operated at 514.5 nm (green line). The cross-beam half angle between the two transmitted beams was 1.872 degrees, calibrated at far field (~25 ft) via beam separation measurement. The LDV optics had a 750.51 mm focal length. The estimated sample volume cross-section was about 175 microns. The transmitting probe was set at an angle of 4 degrees down relative to the horizontal plane to accommodate getting the sample volume into the slot at 0 mm height without blocking the lower beam. The receiving probe was set at an angle of 10 degrees down to ensure that all available scattered light was collected unobstructed.

The probes were mounted on translation stages to provide lateral and vertical motion. The stages have a position accuracy of 1 micron. Once alignment was achieved between the transmission and receiving probes, each was moved individually to each new position. Alignment was ensured by the signal from the photomultiplier tube.

LDV signals from the scattering particles were processed using FFT processors. Doppler frequency, hence velocity signal, was estimated based on 256 point FFT spectrum analysis at each particle arrival. Drive signal waveform was also recorded at the particle arrival time to determine the phase information of the velocity signal.

At each station, 30,000 data points were collected in a period of several minutes, depending on the seeding density. Based on the phase information collected at each data point, 30,000 data were sorted into 36 phase bins, at 10 degree of phase interval. Within each bin, number of samples may vary from a few hundreds to over 2000. Theses samples were used to compute phase-locked statistics.

The uncertainty in the data was calculated using estimates of bias and precision errors in the experiment. The estimates were based on a nominal condition using an approximate mean velocity in the jet. The bias estimates were based on experimental geometrical parameters, LDV processor bias, and biases related to the seeding material used. The total bias and the precision were propagated through the coordinate transformation due to the probe downward tilt and combined to give an estimate of the total uncertainty in the vertical velocity measured of +/- 0.54 m/sec.

Particle Image Velocimetry measurements

PIV measures an instantaneous velocity field over a grid of points in a plane in the fluid. In this test, a Digital PIV system was set up to measure the horizontal and vertical velocity components synchronized with the 445 Hz drive signal. The current PIV system includes 1024 x 1280 CCD cameras installed with a 200mm Nikon Macro lens. The camera lens was placed approximately 12” from the laser sheet to cover a field of view about 9 mm wide. The magnification of the imaging optics was calibrated with an optical grid target aligned with the laser sheet. The accuracy of calibration was within +/-1 pixel over 1240 pixels. Interrogation resolution was set at 28 by 28 pixels corresponding to about 0.2 mm of measurement area.

Dual Nd-Yag lasers, operated at 5 Hz rate and 100 mJ output per pulse, were used to illuminate a light sheet less than 0.5 mm thick. The laser light sheet was projected perpendicular to the slot at the mid–section of the jet slot. Laser pulse separations (δt between double exposure) were adjusted between 1.1 ~ 8.0 μsecond at each phase to maximize PIV performance (8 pixels of maximum particle displacement). In general, PIV resolves between 1/10 and 1/20 sub-pixel resolution.

Both smoke and polystyrene latex spheres particles were used to seed the entire glass enclosure. PIV measurements normally requires higher seeding density than LDV to ensure its performance. Smoke particles were produced by a smoke generator using standard smoke fluids (specific gravity at 1.022). Smoke particles have a poly-disperse size distribution which may cover from sub-micron to tens of micron while PSL particles were are mono-disperse in size when manufactured. Although some large agglomerated PSL particles may still be present in the flows when sprayed into the test chamber with water-ethanol mixture. Particles larger than 5 μm may not follow the jet flows. There was no particle sizer available at the test for in-situ particle size distribution measurements. Both particle, smoke and PSL, were tested to determine if any effects on the PIV measurements of the jet flows, and there was only slight difference between the velocity profiles measured. The glass enclosure was repeatedly seeded to replenish particle density for PIV measurements. Four hundred PIV images were taken at 72 phases, in 5 degree interval synchronized with the drive signal, to estimate the phase-locked statistics.

Flow Field Measurements

The experiment was conducted separately for the three measurement techniques. A new diaphragm was installed in the actuator for each measurement technique due to actuator failures or changes in the actuator performance. It should be noted that, the actuator used to generate the workshop data (given on the website) was different than the ones used to generate the data given in Figs. 3 and 4. The later actuators generated higher jet velocities. However, the overall trends are similar. Inside the cavity, the temperature might raise 12 ~ 13 degrees F above the ambient air after warm-up and then maintained a steady temperature at that point. Hot-wire tests were conducted in clean air while the enclosure was moderately seeded for LDV, and heavily seeded for PIV test. There was no effect detected of seeding density on cavity pressure waveforms.

The zero mass jet flow consists of a pulse train of high speed fluids projected form the slot accompanied by a pair of vortices. An elongated mean jet emerges when the flow fields are time or ensemble averaged. The maximum jet velocity (Fig. 4) was found slightly above the slot, and its magnitude may be scaled by the peak cavity pressure, $\propto (p_{max})^{1/2}$. In the near fields, there was a close comparison found in the velocity profiles obtained by the LDV and PIV, but their magnitudes were off. Good agreements between the LDV and PIV measurements have been reported in liquid experiments, but the discrepancy found in this test has not been resolved. On the other hand, the hot-wire data showed a faster decay of the jet. In the far fields, however, hot-wire and LDV data matched well. Above the maximum jet velocity, the flow is always in upward motion, i.e., its height, about 4 slot width, defines the upper limit of the suction action.

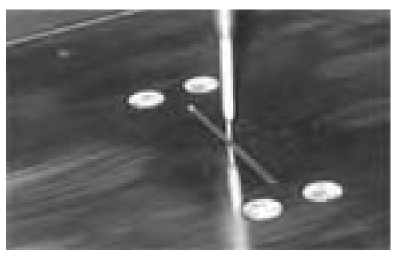

Figure 1: Synthetic jet slot

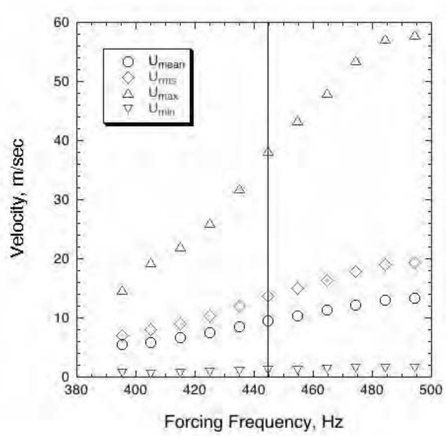

Figure 2: Synthetic jet performance with frequency.

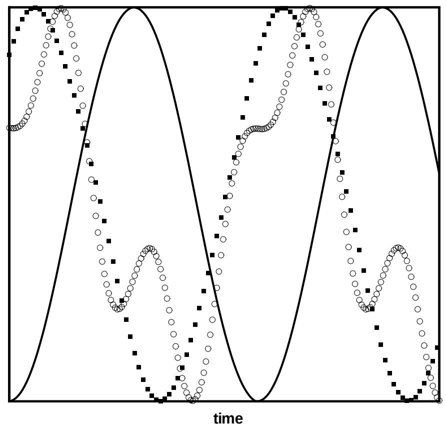

Figure 3: Waveforms of drive signal (line), cavity pressure (circle), and displacement (square).

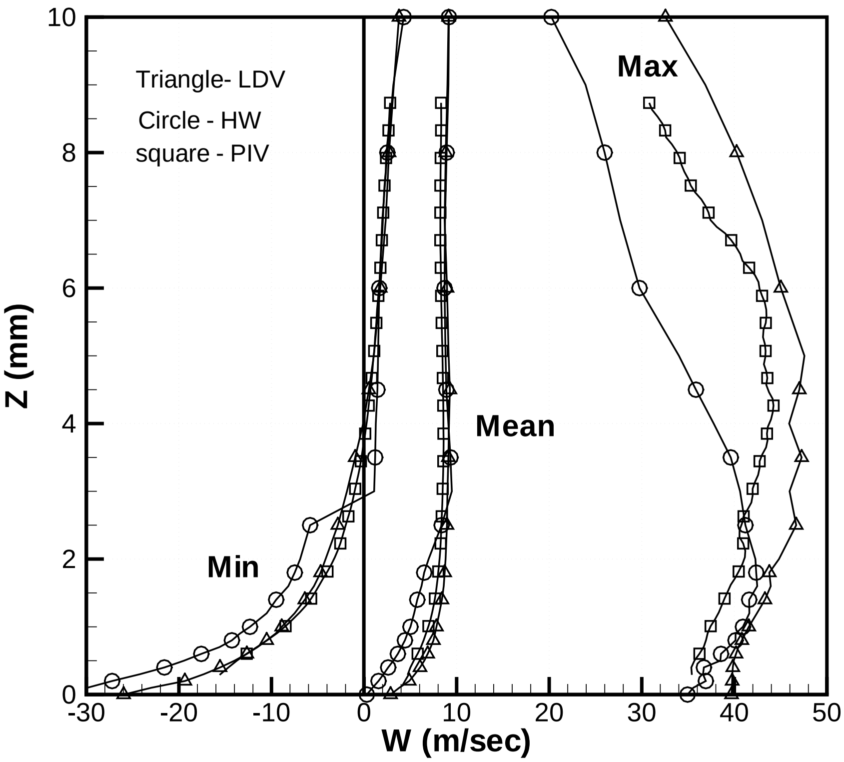

Figure 4: Maximum, minimum and mean velocity profiles.

References

[1] Chen, F.-J., Yao, C., Beeler, G. B., Bryant, R. G., and Fox, R. L., "Development of Synthetic Jet Actuators for Active Flow Control at NASA Langley," AIAA Paper 2000-2405, June 2000.

[2] Chen, F.-J., "Optimized Synthetic Jet Actuators," LAR 16234, NASA Tech Briefs, July 2002